# The doubly excited autoionizing states of $H_2$

Steven L. Guberman

*Boston College, Newton, Massachusetts 02159*[a]
*and Harvard-Smithsonian Center for Astrophysics, Cambridge, Massachusetts 02138*
(Received 23 August 1982; accepted 19 October 1982)

*Ab initio* potential curves have been determined for 24 doubly excited autoionizing states of $H_2$ having primarily the lowest $^2\Sigma_u^+$ and $^2\Pi_u$ states of $H_2^+$ as the core orbital. Fourteen of these states have not appeared previously in the literature. The configuration interaction wave functions are constructed with a Feshbach projection operator formalism. The accuracy of the calculations is assessed by comparison with calculations in the same bases on the lower bound states of $H_2$. The potential curves for the doubly excited states fall into three distinct groups with an energy ordering related to the Hartree energy of the most important configuration of each state. The relative energies of several doubly excited states and the corresponding singly excited bound states of $H_2$ are compared. The grouping of doubly excited states is in good agreement with the electron impact results of Kollman. Both the lowest two states of $Q_1\ ^1\Sigma_u^+$ symmetry and a $Q_2\ ^1\Sigma_u^+$ state with thresholds of 25.5, 27.8, and 33.3 eV, respectively, are important in the interpretation of dissociative photoionization and electron impact experiments. A $Q_2\ ^1\Sigma_g^+$ state with a threshold at 30.2 eV will contribute to the fast H atoms seen in several electron impact experiments.

## I. INTRODUCTION

Neutral doubly excited states of $H_2$ lie in the Franck–Condon region at energies beyond 23 eV above the ground state of $H_2$. These repulsive resonance states may autoionize yielding $H_2^+ + e^-$, $H + H^+ + e^-$ or dissociate to neutral ground and excited H atoms or $H^+ + H^-$. Autoionization to $H_2^+ + e^-$ can lead to an $H_2^+$ ground state vibrational distribution which is considerably different from that arising from direct ionization. Autoionization or dissociation can also lead to atoms with high kinetic energies. These processes are important in determining the thermal balance of interstellar clouds[1] and the chemistry of the Jovian atmosphere.[2]

While production of atomic radiation from electron impact excitation of $H_2$ has been known for many years[3] the mechanisms producing excited H atoms from $H_2$ at thresholds above 23 eV have only been investigated relatively recently. In 1967 Leventhal, Robiscoe, and Lea[4] reported the velocity spectrum of H(2*s*) atoms produced by electron impact of $H_2$ in a time of flight experiment. A threshold at $18 \pm 2$ eV was attributed[5] to dissociation on the repulsive wall of singly excited bound states of $H_2$. An additional threshold at $28.5 \pm 2$ eV was assigned to dissociation along doubly excited states of $H_2$ for which little was known at that time. Observation of the angular distribution of H(2*s*) indicated that more than one doubly excited state was important. Kiefer and Dunn[6] reported disagreement between their calculations and their measurements of the energy spectrum of $H^+$ and $D^+$ produced from electron impact of $H_2$ and $D_2$ at 150 eV. It was suggested that the autoionization of high repulsive states of $H_2$ near the $^2\Sigma_u^+$ state of $H_2^+$ might account for the disagreement.

In 1973 Browning and Fryar[7,8] reported experimental measurements of the $H^+/H_2^+$ ratio arising from excitation of $H_2$ by photons in the range 17.1–30.5 eV. Above the asymptote of $H_2^+ X\,^2\Sigma_g^+$ at 18.08 eV, protons are produced by direct dissociation on the repulsive wall. Near 20 eV the Franck–Condon factor for direct dissociation becomes quite small. The experiments show (in agreement with theoretical calculations[9]) that the $H^+/H_2^+$ ratio increases from zero at 18.08 eV and reaches a plateau near 20 eV. The $H^+/H_2^+$ ratio is expected to increase again near 29 eV where direct photoionization can occur through the $^2\Sigma_u^+$ repulsive state. However, Browning and Fryar found that $H^+/H_2^+$ increased near 26 eV, below the threshold for $^2\Sigma_u^+$. The increase in $H^+/H_2^+$ is due to neutral doubly excited resonance states of $H_2$ lying beneath the $^2\Sigma_u^+$ state. Kollman[10] has reported three threshold regions for production of $H^*$ by electron impact at energies beneath 29 eV. Strathdee and Browning[11,12] have reported measurements of the proton kinetic energy distribution resulting from the dissociative ionization of $H_2$ by 19.8–40.8 eV photons. A recent calculation[13] using the lowest $^1\Sigma_u^+$ autoionizing state reported here shows good agreement with the measurements for the $H^+$ production cross section and the $H^+/H_2^+$ ratio. Several workers[14–18] have reported large widths for the Balmer lines of $H^*$ produced by electron impact dissociative excitation of doubly excited states with thresholds above 23 eV. There has been additional evidence for these doubly excited states in electron impact experiments on $H_2$ or $D_2$ involving observation of atomic emission,[19–21] time of flight spectra of long lived atomic states,[22–26] detection of $H^+$ and/or $D^+$,[27–32] and coincident detection of the decay of two excited atoms arising from a single doubly excited state.[33] In addition, theoretical calculations of a few states have been reported.[34–43]

This paper presents *ab initio* calculations of 24 autoionizing states of $H_2$ which have mostly the $^2\Sigma_u^+$ and first excited $^2\Pi_u$ states of $H_2^+$ as the core orbital near $R = 1.4a_0$. We retain the notation of previous authors[40–42] who have labeled the former states $Q_1$ and the latter $Q_2$. For the $Q_1$ states, the lowest two $^{1,3}\Sigma_{g,u}^+$ and $^{1,3}\Pi_{g,u}$ states have been determined. For the $Q_2$ states, the lowest state of each of these symmetries is presented. In Sec. II, the construction of the wave functions is discussed. In Sec. III, the potential curves are presented.

[a]Current address.

 0021-9606/83/031404-10$2.10 

In Sec. IV, comparison is made to other theoretical results. A discussion of experimental results in light of these calculations is in Sec. V.

## II. METHOD

### A. Wave functions and projection operators

The spatial wave functions are expanded as a sum of products of orthonormal one electron orbitals:

$$\Psi = \sum_{i \geq j}^{n} C_{ij} \{\phi_i(1)\phi_j(2)\} . \quad (1)$$

For $i=j$ the brackets in Eq. (1) denote a simple product of orbitals while for $i \neq j$ we have

$$\{\phi_i(1)\phi_j(2)\} = \frac{1}{\sqrt{2}} (\phi_i(1)\phi_j(2) \pm \phi_j(1)\phi_i(2)) ,$$

where the upper sign is taken for singlets and the lower sign for triplets. The $C_{ij}$ are variationally optimum configuration interaction (CI) coefficients obtained by diagonalizing the electronic Hamiltonian matrix constructed over the configurations in Eq. (1).

At intermediate internuclear distances $R$ each resonance state described here lies above an infinite number of neutral states of the same symmetry having the ground state of $H_2^+$ as the series limit. This infinite set of states is excluded by partitioning the space of the full Hamiltonian. The Feshbach projection operator formalism originally developed for nucleon–nucleus[44] scattering is employed here. The application of this formalism to electron–atom[45] and electron–molecule[35,46] scattering has been described elsewhere and is only briefly summarized here. Two projection operators $P_1$ and $Q_1$ are defined such that $P_1$ projects onto all electronic states described by the ground state of the target ($H_2^+$, $X\,^2\Sigma_g$) plus a captured or scattered electron and $Q_1$ projects onto the remaining electronic states. The $Q_1$ compound states, described at the end of the previous section, consist of an excited target primarily in the $^2\Sigma_u^+$ state and a captured projectile electron. Similarly, $P_2$ and $Q_2$ can be defined such that $P_2$ projects onto all electronic states of the ground and first excited state ($^2\Sigma_u^+$) of the target plus a captured or scattered electron. The $Q_2$ compound states consist of an excited target mostly in the $^2\Pi_u$ state and a captured projectile electron. The projection operators lead to coupled equations which can be uncoupled resulting in a one body equation for $P_n\Psi$. The two body effects appear in a generalized optical potential which is singular at the energies of the autoionizing or resonance states. The energies of these resonances are the eigenvalues of $Q_nHQ_n$. Associated with each resonance is an energy shift and width due to interaction with $P$ space. The resonance energies are given by $E_m = \epsilon_m + \Delta_m$ where $\epsilon_m$ is an eigenvalue of $Q_nHQ_n$ and $\Delta_m$ is a shift due to the interaction of $Q_n\Psi$ with states that have been projected out of $Q_n$ space. If the operator $Q_n$ allows for the inclusion in $Q_n\Psi$ of all the important configurations needed to describe the resonance state the shift $\Delta_m$ will be small. Also associated with each resonance is a width which is proportional to the square of matrix elements of $P_nHQ_n$. The width is a measure of the probability for decay of the resonance to the states of $P_n$ space. The reader is referred to Refs. 35, 44, 45, and 46 for a more detailed discussion of the energy shift and the width.

For $H_2$ we take $P_1(1) = |1\sigma_g(1)\rangle\langle 1\sigma_g(1)|$ and $Q_1(1) = 1 - P_1(1)$, where $1\sigma_g$ is the exact one electron wave function for the ground state of $H_2^+$. The two electron projection operator is given by

$$P_1(1,2) = P_1(1) + P_1(2) - P_1(1)P_1(2) . \quad (2)$$

In order to describe the compound autoionizing states, we apply the operator

$$Q_1(1,2) = Q_1(1)Q_1(2) = 1 - P_1(1,2)$$

to the wave function in Eq. (1). If $\Psi$ is expanded over exact one electron wave functions of $H_2^+$, $Q_1(1,2)\Psi$ does not contain the $1\sigma_g$ orbital. Similarly we have

$$P_2(1) = |1\sigma_g(1)\rangle\langle 1\sigma_g(1)| + |1\sigma_u(1)\rangle\langle 1\sigma_u(1)|$$

with $Q_2(1) = 1 - P_2(1)$. $Q_2(1,2)\Psi$ does not contain the $1\sigma_g$ and $1\sigma_u$ orbitals.

In order to obtain a variationally optimum $Q_n\Psi$ it is necessary to optimize the eigenvalues of $Q_nHQ_n$. This is equivalent to finding the eigenvalues of H if the matrix elements of H are only those between the configurations found in $Q_n\Psi$.[27] The Hylleraas, Undheim, and McDonald theorem[47] applies to $Q_nHQ_n$ as it does to H. The $i$th root of $Q_nHQ_n$ will be an upper bound to the $i$th exact autoionizing state in $Q_n$ space as long as the exact $H_2^+$ states are projected out of $Q_n$ space. As the number of configurations is increased or as the basis set is improved the eigenvalues approach the exact eigenvalues. The lowest autoionizing state will be the first root of the $Q_nHQ_n$ CI matrix. In other approaches, such as the stabilization method, the lowest autoionizing state will correspond to an excited root of the Hamiltonian matrix.

### B. Basis set

Because of the nature of the projection operators used here it is most convenient to use optimized $H_2^+$ orbitals for the $\phi_i$ in Eq. (1). $Q_1\Psi$ is obtained by simply eliminating the $1\sigma_g$ orbital from Eq. (1). $Q_2\Psi$ is obtained by eliminating both the $1\sigma_g$ and $1\sigma_u$ orbitals. Higher $Q_n\Psi$ states are obtained by eliminating additional $H_2^+$ orbitals. In order to be certain that we have an accurate description of the $Q_n$ states, it is necessary to have accurate descriptions of the one electron states of $H_2^+$. The basis set used here consists of Gaussian primitive functions[48] contracted into groups of functions with scales optimized for the one electron orbitals of $H_2^+$. Since we are primarily interested in the internuclear separation spanned by the Franck–Condon region of $v=0$ of the ground state of $H_2$ the basis set contractions were optimized at $R = 1.4a_0$. The two basis sets used in this work are shown in Table I. The $Q_1$ states of $g$ symmetry consist primarily of the $2p\sigma_u(1\sigma_u)$ core orbital plus excited orbitals of $u$ symmetry. In the Franck–Condon region, the $g$ basis of Table I provides accurate descriptions of $H_2^+$ $1s\sigma_g$, $2s\sigma_g$, $3s\sigma_g$, $2p\sigma_u$, $3p\sigma_u$, $4p\sigma_u$, $2p\pi_u$, $3p\pi_u$, and $4f\pi_u$ orbitals. The $Q_1$ states of $u$ symmetry consist mostly

TABLE I. Gaussian basis set.

| Exponents | Type[a] | Contraction coefficients: g basis | Contraction coefficients: u basis[b] |
|---|---|---|---|
| 82.474 | | 0.005 535 2 | g |
| 12.398 | | 0.044 669 7 | g |
| 2.839 1 | | 0.193 75 | g |
| 0.814 72 | s | 0.824 46 | g |
| 0.271 84 | | 1.0 | g |
| 0.099 483 | | 1.0 | g |
| 0.582 74 | | ··· | 0.106 00 |
| 0.042 726 | | 1.0 | −1.033 1 |
| 0.016 5 | | 1.0 | g |
| 1.253 48 | | 0.535 02 | g |
| 0.291 528 | | 0.603 34 | g |
| 0.022 284 | z | −1.098 6 | ··· |
| 0.005 182 7 | | 0.211 41 | ··· |
| 2.377 5 | | −0.019 51 | ··· |
| 0.564 44 | | −0.188 16 | ··· |
| 0.180 51 | | −0.564 35 | ··· |
| 0.065 399 | | −0.374 95 | ··· |
| 1.056 70 | | ··· | 0.003 774 0 |
| 0.250 86 | | ··· | 0.068 481 |
| 0.080 227 | x, y | ··· | 0.461 70 |
| 0.029 066 | | ··· | 0.572 13 |
| 0.341 96 | | −0.038 295 | ··· |
| 0.033 519 | | 1.008 7 | 0.145 78 |
| 0.016 222 | | 1.0 | 0.872 98 |
| 0.007 350 5 | | 1.0 | 1.0 |
| 0.003 330 7 | | ··· | 1.0 |
| 0.819 29 | | ··· | −0.017 708 |
| 0.220 39 | xx, yy, zz | ··· | −0.213 55 |
| 0.078 899 | | ··· | −0.529 90 |
| 0.031 799 | | ··· | −0.412 92 |

[a] s indicates a 1s Gaussian primitive while x, y, z indicates 2p primitives and xx, yy, zz indicate 3d primitives.
[b] A g indicates that the same primitives and contraction coefficients are used in the u basis as in the g basis.

of the $2p\sigma_u$ core orbital plus excited orbitals of g symmetry. The u basis provides accurate descriptions of $H_2^+$ $1s\sigma_g$, $2p\sigma_u$, $2s\sigma_g$, $3d\sigma_g$, $3s\sigma_g$, $3d\pi_g$, $4d\pi_g$, and $5g\pi_g$ orbitals. Generally, it was found that the g $Q_1$ states had lower energies in the g basis while the u $Q_1$ states had lower energies in the u basis. Two exceptions are $Q_1\,{}^3\Sigma_u^+(2)$[50] and $Q_1\,{}^1\Sigma_u^+(2)$ which are described in the g basis. The diffuse $2p_z$ functions of the g basis are important in both of these states. Each of the bases in Table I yield seven $\sigma_g$, seven $\sigma_u$, four $\pi_{gx}$, four $\pi_{gy}$, four $\pi_{ux}$, and four $\pi_{uy}$ $H_2^+$ orbitals. The $\sigma_g$ and $\sigma_u$ orbitals with the highest one electron energies were energetically unimportant in the two electron states and were eliminated. For each spatial and spin symmetry the wave functions consisted of a full CI over these 12 $\sigma$ orbitals and 16 $\pi$ orbitals leading to wave functions having between 44 and 76 terms. The calculated $1\sigma_g$ and $1\sigma_u$ $H_2^+$ orbital energies are compared to exact energies in Table II. The average error for $1\sigma_g$ and $1\sigma_u$ over the range $R = 1.0$–$4.0a_0$ is only 0.028 eV. In the calculations reported here all $Q_1$ states of u symmetry [except for ${}^3\Sigma_u^+(2)$ and ${}^1\Sigma_u^+(2)$] are described in the u basis while all $Q_1$ states of g symmetry are described in the g basis. For the $Q_2$ states both the $1\sigma_g$ and $1\sigma_u$ orbitals are projected out of the CI wave function and the $2p\pi_u$ $H_2^+$ orbital is the core at internuclear distances near $R = 1.4\,a_0$. This orbital is described better by the g basis than the u basis. Tests showed that the energies of the $Q_2$ states in the g basis were lower than energies in the u basis. The g basis has been used for the description of all eight $Q_2$ states discussed here.

In order to assess the accuracy of the basis sets shown in Table I calculations were performed on the lower bound states of $H_2$. The wave functions consisted of a full CI over the previously described orbitals with the inclusion of the $1\sigma_g$ orbital. Except for the $h\,{}^3\Sigma_g^+$ and the $G$, $K\,{}^1\Sigma_g^+$ states [the analogs of $Q_1\,{}^3\Sigma_u^+(2)$ and ${}^1\Sigma_u^+(2)$] the calculations for the g bound states were done in the u basis while all u bound states were done in the g basis. This is required by the switch in symmetry of the core orbital which is $1\sigma_g$ for the lower bound states but $1\sigma_u$ for the $Q_1$ states. Experimental results and the calculations of Kolos and Wolniewicz allow a comparison to very accurate energies for ten of the states shown in Table III. For these ten states the average difference between these calculations and the very accurate results is only 0.08 eV. The $h\,{}^3\Sigma_g^+$ state is described the poorest and is 0.3 eV above the calculation by Wakefield and Davidson.[49] Except for the h state the results are quite encouraging. We can expect the $Q_1$ states to be accurate to better than about 0.2 eV except for possibly the second root of ${}^3\Sigma_u^+$ symmetry (the $Q_1$ analog of $h\,{}^3\Sigma_g^+$).

## III. RESULTS

The calculated energies for the $Q_1$ and $Q_2$ states are listed in Tables IV and V, respectively, and the potential curves are shown in Fig. 1. All the curves are repulsive with the $Q_1$ and $Q_2$ states nearly parallel to the core ${}^2\Sigma_u^+$ and ${}^2\Pi_u$ states of $H_2^+$ respectively. Thresholds, i.e. vertical excitation energies at $R = 1.8a_0$, of the

TABLE II. Calculated electronic energies for the $1\sigma_g$ and $1\sigma_u$ $H_2^+$ orbitals.[a]

| $R$[b] | $E$[c] $1\sigma_g$ | $E$[c] $1\sigma_u$ | $\Delta E$[d] $1\sigma_g$ | $\Delta E$[d] $1\sigma_u$ |
|---|---|---|---|---|
| 1.0 | −1.449 44 | −0.564 29 | 0.002 34 | 0.000 52 |
| 1.2 | −1.361 25 | −0.588 20 | 0.001 05 | 0.000 41 |
| 1.4 | −1.283 66 | −0.611 83 | 0.000 60 | 0.000 24 |
| 1.6 | −1.215 44 | −0.633 45 | 0.000 49 | 0.000 15 |
| 1.8 | −1.155 23 | −0.652 08 | 0.000 58 | 0.000 15 |
| 2.0 | −1.101 84 | −0.667 36 | 0.000 78 | 0.000 17 |
| 2.5 | −0.991 84 | −0.691 80 | 0.001 97 | 0.000 27 |
| 3.0 | −0.907 43 | −0.701 08 | 0.003 46 | 0.000 33 |
| 4.0 | −0.791 51 | −0.695 11 | 0.004 57 | 0.000 44 |

[a] All energies are in hartrees.
[b] All distances are in bohr.
[c] The energies listed are for the u basis of Table I. Results with the g basis differ at all distances by less than 0.0002 hartrees from the energies listed here.
[d] $\Delta E$ is the difference between the exact energies and the calculated energies. The exact energies have been taken from D. R. Bates, K. Ledsham, and A. L. Stewart, Proc. R. Soc. London 246, 215 (1953); and M. M. Madsen and J. M. Peak, At. Data 2, 171 (1971).

TABLE III. Energies for singly excited states of $H_2$.[a]

| State | This calculation[b] | Previous studies | Column 2–column 3 |
|---|---|---|---|
| $b\,^3\Sigma_u^+$ | −0.78196 | −0.7841501[c] | 0.00219 |
| $e\,^3\Sigma_u^+$ | −0.64266 | −0.6414[d] | −0.0012 |
| $c\,^3\Pi_u$ | −0.70354 | −0.7027[d] | −0.0008 |
| $d\,^3\Pi_u$ | −0.62732 | −0.6291[d] | 0.0018 |
| $C\,^1\Pi_u$ | −0.68488 | −0.6885[e] | 0.0037 |
| $D\,^1\Pi_u$ | −0.62156 | −0.6233710,[f] −0.6254[g] | 0.00181, 0.0038 |
| $B\,^1\Sigma_u^+$ | −0.70163 | −0.7057434[h] | 0.00411 |
| $a\,^3\Sigma_g^+$ | −0.71199 | −0.7136358[h] | 0.00164 |
| $h\,^3\Sigma_g^+$ | −0.61797 | −0.62995[i] | 0.01198 |
| $i\,^3\Pi_g$ | −0.62533 | −0.62609[j] | 0.00076 |
| $E, F\,^1\Sigma_g^+$ | −0.68981 | −0.6919[k] | 0.0021 |
| $G, K\,^1\Sigma_g^+$ | −0.61682 | −0.6254[l] | 0.0086 |

[a]All energies are in hartrees and are for $R = 1.4a_0$.
[b]All $u$ state energies are calculated in the $g$ basis and all $g$ state energies are calculated in the $u$ basis shown in Table I. The only exceptions are $h\,^3\Sigma_g$ and $G, K\,^1\Sigma_g$ which were obtained in the $g$ basis (see the text).
[c]W. Kolos and L. Wolniewicz, J. Chem. Phys. 43, 2429 (1965).
[d]The energy is from a quartic fit to the data in G. H. Dieke, J. Mol. Spectrosc. 2, 494 (1958).
[e]This is from a quartic fit to the energies given in footnote c.
[f]S. Rothenberg and E. R. Davidson, J. Chem. Phys. 44, 730 (1966).
[g]From a quartic fit to the energies given in R. J. Spindler, Jr., J. Quant. Spectrosc. Radiat. Transfer 9, 627 (1969).
[h]W. Kolos and L. Wolniewicz, J. Chem. Phys. 48, 3672 (1968).
[i]From Ref. 49.
[j]W. M. Wright and E. R. Davidson, J. Chem. Phys. 45, 515 (1966).
[k]The energy is from a quartic fit to the data in W. Kolos and L. Wolniewicz, J. Chem. Phys. 50, 3228 (1969).
[l]The energy is from a quartic fit to the data in Ref. 52.

resonances above $v'' = 0$, $X\,^1\Sigma_g^+$ are listed in Table VI. Energetically the states fall into three distinct groups. The lowest state $^1\Sigma_g^+(1)$ crosses the right edge of the Franck–Condon region of the ground state of $H_2$ ($R = 1.8a_0$) at 23.0 eV above $v'' = 0$ and is 2.2 eV below the next accessible state, $^3\Sigma_u^+(1)$. The calculated curve also crosses the large $R$ turning point of the $v = 1$ level of $H_2^+\,^2\Sigma_g^+$. The $^1\Sigma_g^+$ state at low electron energies is therefore the most important doubly excited state for dissociative recombination of the lower vibrational levels of $H_2^+$.

At higher energies a second group of states consisting of $^3\Sigma_u^+(1)$, $^3\Pi_g(1)$, $^1\Sigma_u^+(1)$, and $^1\Pi_g(1)$ become accessible. The $^1\Sigma_u^+$ state is 25.5 eV above $v'' = 0$ of $X\,^1\Sigma_g^+$ at $R = 1.8a_0$ and is the lowest dipole allowed resonance.

The third group of states includes all of the remaining calculated $Q_1$ states and is the region shown by the vertical lines in Fig. 1, bounded by the $^1\Sigma_g^+(2)$ state and the highest calculated $Q_1$ state $^3\Pi_u(2)$.

The energetic partitioning of these states into three groups can be qualitatively understood by neglecting the electron–electron repulsion energy and simply adding together the one electron orbital energies in the most important configuration of each state. For $^1\Sigma_g^+(1)$ we obtain (at $R = 1.4a_0$) $E(1\sigma_u) + E(1\sigma_u) = -1.22$ hartree. In the second group of states we obtain $E(1\sigma_u) + E(1\pi_u) = -1.06$ hartree for $^{3,1}\Pi_g(1)$ and $E(1\sigma_u) + E(2\sigma_g) = -1.00$ hartree for $^{3,1}\Sigma_u(1)$. For the third group of states the sum of the orbital energies ranges from −0.86 to −0.74 hartree. The $Q_1$ states are energetically partitioned into three groups because of the predominance of one or two configurations in describing each state. Also the exchange interaction does not vary significantly enough from state to state and is not large enough to cause singlet–triplet splittings to disturb the groupings. Indeed, a similar approach can be used for the lower bound states of $H_2$. The nearly degenerate $Q_1\,^3\Sigma_u^+(1)$ and $^3\Pi_g(1)$ states have as their counterparts (upon replacing $1\sigma_u$ by $1\sigma_g$) the $a\,^3\Sigma_g^+$ and $c\,^3\Pi_u$ lower bound states. The latter two states are nearly degenerate near their minima. Similarly the nearly degenerate $Q_1\,^1\Sigma_u^+(1)$ and $^1\Pi_g(1)$ states have as their counterparts the $E, F\,^1\Sigma_g^+$ state and the $C\,^1\Pi_u$ state. The latter two states are nearly degenerate near the inner minimum of $E, F\,^1\Sigma_g^+$. The $B\,^1\Sigma_u^+$ state could be taken to be the counterpart of $Q_1\,^1\Sigma_g^+(1)$, however, the exchange interaction between the $1\sigma_g$ and $1\sigma_u$ orbitals leads to a large splitting at intermediate $R$ dropping $b\,^3\Sigma_u^+$ and raising $B\,^1\Sigma_u^+$.

Because the $1\sigma_g$ orbital has been projected out of the wave function, the $Q_1$ states dissociate to a super-

TABLE IV. Energies of the $Q_1$ states.[a]

| $R$ | $^1\Sigma_g^+(1)^b$ | $^1\Sigma_g^+(1)^c$ | $^1\Sigma_g^+(1)^d$ | $^1\Sigma_g^+(1)$ | $^3\Sigma_u^+(1)^b$ | $^3\Sigma_u^+(1)$ | $^3\Pi_g(1)$ | $^1\Pi_g(1)$ | $^1\Sigma_u^+(1)^c$ |
|---|---|---|---|---|---|---|---|---|---|
| 1.0 | 0.2401 | 0.259 | 0.274077 | 0.24343 | 0.2539 | 0.25198 | 0.26414 | 0.28078 | 0.315 |
| 1.2 | 0.0473 | ··· | 0.070871 | 0.04827 | 0.0775 | 0.07538 | 0.08202 | 0.09883 | ··· |
| 1.4 | −0.0990 | ··· | ··· | −0.10162 | −0.0536 | −0.05588 | −0.05347 | −0.03691 | ··· |
| 1.6 | −0.2169 | ··· | −0.204892 | −0.22083 | −0.1554 | −0.15768 | −0.15837 | −0.14236 | ··· |
| 1.8 | ··· | ··· | ··· | −0.31752 | ··· | −0.23847 | −0.24142 | −0.22610 | ··· |
| 2.0 | −0.3900 | −0.379 | −0.383751 | −0.39688 | −0.3013 | −0.30336 | −0.30801 | −0.29340 | −0.283 |
| 2.5 | −0.5320 | ··· | −0.529237 | −0.54035 | −0.4151 | −0.41662 | −0.42412 | −0.41103 | ··· |
| 3.0 | −0.6223 | −0.595 | −0.621048 | −0.63074 | −0.4834 | −0.48462 | −0.49366 | −0.48177 | −0.470 |
| 4.0 | −0.7175 | −0.658 | −0.716708 | −0.72569 | −0.5495 | −0.55210 | −0.56115 | −0.55105 | −0.537 |
| 6.0 | −0.7666 | −0.648 | ··· | −0.77762 | −0.5807 | −0.58907 | −0.59165 | −0.58410 | −0.574 |

| $R$ | $^1\Sigma_u^+(1)$ | $^3\Sigma_g^+(1)$ | $^1\Sigma_g^+(2)$ | $^3\Pi_g(2)$ | $^1\Pi_g(2)$ | $^3\Pi_u(1)^b$ | $^3\Pi_u(1)$ | $^1\Pi_u(1)$ |
|---|---|---|---|---|---|---|---|---|
| 1.0 | 0.28600 | 0.35543 | 0.35689 | 0.36956 | 0.37167 | 0.3431 | 0.37913 | 0.37832 |
| 1.2 | 0.10132 | 0.16378 | 0.18121 | 0.18085 | 0.18354 | 0.1788 | 0.18617 | 0.18908 |
| 1.4 | −0.03604 | 0.02002 | 0.03595 | 0.03977 | 0.04287 | 0.0427 | 0.04488 | 0.04684 |
| 1.6 | −0.14222 | −0.09180 | −0.07606 | −0.06974 | −0.06641 | −0.0669 | −0.06571 | −0.06390 |
| 1.8 | −0.22609 | −0.18057 | −0.16516 | −0.15661 | −0.15317 | ··· | −0.15368 | −0.15192 |
| 2.0 | −0.29313 | −0.25190 | −0.23690 | −0.22639 | −0.22292 | −0.2253 | −0.22451 | −0.22276 |
| 2.5 | −0.40929 | −0.37681 | −0.36290 | −0.34864 | −0.34522 | −0.3500 | −0.34915 | −0.34731 |
| 3.0 | −0.47826 | −0.45249 | −0.43952 | −0.42278 | −0.41949 | −0.4264 | −0.42545 | −0.42340 |
| 4.0 | −0.54516 | −0.52819 | −0.51676 | −0.49717 | −0.49414 | −0.5051 | −0.50375 | −0.50105 |
| 6.0 | −0.57896 | −0.56814 | −0.55834 | −0.53736 | −0.53474 | −0.5515 | −0.55053 | −0.54653 |

| $R$ | $^3\Sigma_u^+(2)$ | $^1\Sigma_u^+(2)$ | $^3\Sigma_g^+(2)$ | $^3\Pi_u(2)$ | $^1\Pi_u(2)^e$ | $^1\Pi_u(2)^f$ | $^1\Pi_u(2)$ |
|---|---|---|---|---|---|---|---|
| 1.0 | 0.37669 | 0.38191 | 0.40125 | 0.37913 | 0.3837 | ··· | 0.40258 |
| 1.2 | 0.19082 | 0.19437 | 0.20983 | 0.21380 | 0.2285 | 0.2132 | 0.21347 |
| 1.4 | 0.05216 | 0.05342 | 0.06637 | 0.07009 | 0.1200 | 0.07077 | 0.07115 |
| 1.6 | −0.05713 | −0.05661 | −0.04515 | −0.04057 | 0.0370 | −0.03979 | −0.03962 |
| 1.8 | −0.14508 | −0.14428 | −0.13368 | −0.12857 | ··· | ··· | −0.12765 |
| 2.0 | −0.21611 | −0.21497 | −0.20484 | −0.19940 | −0.1052 | −0.1986 | −0.19847 |
| 2.5 | −0.34149 | −0.33959 | −0.32960 | −0.32392 | −0.2267 | −0.3231 | −0.32294 |
| 3.0 | −0.41882 | −0.41619 | −0.40539 | −0.40002 | −0.3026 | −0.3990 | −0.39893 |
| 4.0 | −0.50034 | −0.49590 | −0.48145 | −0.47775 | −0.3822 | −0.4758 | −0.47638 |
| 6.0 | −0.55635 | −0.54938 | −0.52046 | −0.52326 | −0.4421 | −0.5170 | −0.52142 |

[a]All energies are in hartrees and distance ($R$) in bohr. The number in parentheses after the state symbol denotes the first or second root of that symmetry.
[b]Reference 42.
[c]Reference 35.
[d]Reference 55.
[e]Reference 40.
[f]Reference 38.

position of $H^+$ and $H^-(1s, nl)$ and $H(1s)+H(nl)$. If appropriate configurations occupying the $1\sigma_g$ orbital are included in the wave function these resonance states will dissociate to $H^+ + H^-$. However, except for $^1\Sigma_g^+(1)$ the $H^-$ ions will correspond to $H^-(1s, 2s)$, $H^-(1s, 2p)$, etc. These states have very large widths for decay to $H(1s)+e^-$. Any attempt to variationally optimize the outer orbital would lead to an increasingly diffuse orbital which would eventually describe a free electron. Obtaining the optimum description of these $Q_1$ states at large $R$ would be difficult. Furthermore, recent calculations[13] on the $Q_1\,{}^1\Sigma_u^+$ state show that 97% of the state autoionizes to $H_2^+ + e^-$ or $H^+ + H + e^-$ before crossing beneath the $H_2^+$ ground state potential curve at $R=4.0a_0$. A calculation[37] of autoionization from $^1\Sigma_g^+(1)$ shows that 86% of this state autoionizes before reaching the crossing point. In this paper we are concerned primarily with the region $R<4.0\ a_0$. In separate calculations at $R=1.4\ a_0$ the author has found that the difference between the $Q_1$ states reported here and states including configurations occupying the $1\sigma_g$ orbital (upper roots from the calculations shown in Table III) is in general less than 0.1 eV.[51] This is an indication of the unimportance (in the Franck–Condon region) of $P$ space configurations excluded from the $Q$ space resonance states defined here.

Since both the $1\sigma_g$ and $1\sigma_u$ orbitals are projected out of the $Q_2$ states, these states dissociate to neutral excited H atoms, i.e., $H(nl)+H(n'l')$.

Note that the $Q_1\,{}^1\Sigma_g^+(1)$ state is energetically precisely in the region needed to account for the outer minimum in the $E$, $F$ and $G$, $K$ states in addition to the small perturbations in the $H$, $\bar{H}$ and higher $^1\Sigma_g^+$ states reported by Wolniewicz and Dressler.[52] The $(1\sigma_u)^2$ configuration, a major component of this $Q_1$ state, has been previously identified[53] as the origin of these double minima and perturbations.

TABLE V. Energies for $Q_2$ states.

| $R$ | $^3\Pi_u$ | $^1\Sigma_g$ | $^1\Pi_u$ [b] | $^1\Pi_u$ | $^1\Pi_g$ | $^3\Pi_g$ | $^3\Sigma_g$ | $^3\Sigma_u$ | $^1\Sigma_u$ |
|---|---|---|---|---|---|---|---|---|---|
| 1.0 | 0.322 78 | 0.327 44 | 0.3857 | 0.387 66 | 0.443 95 | 0.444 66 | 0.449 96 | 0.461 49 | 0.467 60 |
| 1.2 | 0.173 63 | 0.178 24 | 0.2390 | 0.233 31 | 0.283 40 | 0.284 40 | 0.293 56 | 0.302 92 | 0.309 99 |
| 1.4 | 0.071 59 | 0.075 54 | 0.1241 | 0.126 84 | 0.171 09 | 0.172 39 | 0.185 14 | 0.192 08 | 0.200 34 |
| 1.6 | −0.001 26 | 0.001 74 | 0.0464 | 0.050 25 | 0.089 13 | 0.090 70 | 0.106 74 | 0.111 05 | 0.120 70 |
| 1.8 | −0.054 88 | −0.052 93 | ··· | −0.006 49 | 0.027 49 | 0.029 32 | 0.048 33 | 0.049 84 | 0.061 02 |
| 2.0 | −0.095 20 | −0.094 37 | −0.0565 | −0.049 43 | −0.019 91 | −0.017 85 | 0.003 84 | 0.002 44 | 0.015 22 |
| 2.5 | −0.159 65 | −0.161 59 | −0.1306 | −0.118 86 | −0.099 00 | −0.096 42 | −0.068 99 | −0.077 86 | −0.061 04 |
| 3.0 | −0.194 85 | −0.199 19 | −0.1733 | −0.157 45 | −0.145 40 | −0.142 36 | −0.110 24 | −0.126 53 | −0.106 07 |
| 4.0 | −0.229 38 | −0.236 38 | −0.2184 | −0.195 08 | −0.193 80 | −0.189 72 | −0.150 89 | −0.181 32 | −0.156 20 |
| 6.0 | −0.260 24 | −0.265 76 | −0.2415 | −0.223 08 | −0.230 95 | −0.222 21 | −0.198 86 | −0.231 30 | −0.210 34 |

[a] Distances ($R$) are in bohr and energies are in hartrees. [b] Reference 40.

## IV. COMPARISON TO PREVIOUS CALCULATIONS

Of the 24 states reported here, 14 have not appeared previously in the literature. For four of the remaining ten states an energy at only a single internuclear distance has been previously reported. Tables IV and V include the potential curves of the five $Q_1$ states and one $Q_2$ state reported previously. All the previous projected calculations [except for $^1\Sigma_g^+(1)$ in Ref. 35] have used the same definition of the $P$ and $Q$ projection operators used here. The $Q_1\,^1\Sigma_g^+(1)$ state reported by Bottcher and Docken[42] is about 0.09 eV below the current energies at small $R$ and about 0.2 eV above the current results near the crossing with $H_2^+\,X\,^2\Sigma_g^+$ and at larger $R$. The curve reported here crosses the ground state of $H_2^+$ at $R = 2.72\ a_0$ compared to $R = 2.8\ a_0$.[41] Excluding consideration of the electronic width the curve reported here would give cross sections for direct dissociative recombination into $v = 1$ which are about 2–3 times larger than that previously reported.[41] The peak vibrational overlap for direct dissociative recombination of $v = 0$ $^2\Sigma_g^+$ through the $^1\Sigma_g^+$ state will come at an electron energy of about 6 eV. The next accessible states are the $^3\Sigma_u^+(1)$ and $^3\Pi_g(1)$ states at about 8.5 eV. At thermal electron energies dissociative recombination of the levels $v \gtrsim 1$ can occur via $^1\Sigma_g^+(1)$. The next accessible routes at thermal energies are $^3\Sigma_u^+(1)$ and $^3\Pi_g(1)$ for $v \geq 6$. The potential curve reported by O'Malley[35] is a qualitative description and consists of a six configuration calculation which included the $1\sigma_g^2$ term. The latter term results in dissociation to $H^+ + H^-$ leading to higher energies than the current results at very large $R$. However, use of a more extended wave function would probably lower O'Malley's result to the current results in the range $R = 1.0$–$3.0\ a_0$ (see Sec. III). Moiseyev and Corcoran[54] have recently reported a complex scaling calculation of the energy and width of $Q_1\,^1\Sigma_g^+$ at $R = 1.4\ a_0$. They report $E = -0.0967$ hartree which is in good

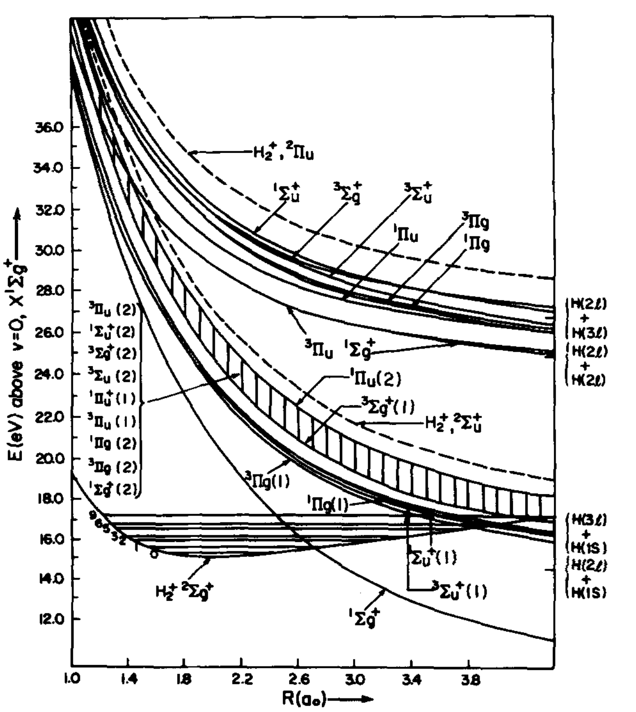

FIG. 1. The potential energy curves of the $Q_1$ and $Q_2$ autoionizing states of $H_2$. The $Q_1$ states are labeled by a (1) or (2) indicating the first or second root of that symmetry. For the $Q_2$ states only the lowest root of each symmetry is shown. The ground state of $H_2^+$ and the $^2\Sigma_u^+$ and $^2\Pi_u$ excited states (dashed lines) are also shown. A closely spaced group of $Q_1$ states bounded by $^3\Sigma_g^+(1)$ and $^1\Pi_u(2)$ is shown with vertical lines. These states are labeled in the bracket on the left of the figure in order of increasing energy at $R = 1.4\ a_0$.

TABLE VI. Thresholds for the autoionizing states.[a]

| $Q_1$ states | | | | $Q_2$ states | |
|---|---|---|---|---|---|
| State | Threshold (eV) | State | Threshold (eV) | State | Threshold (eV) |
| $^1\Sigma_g^+(1)$ | 23.0 | $^1\Pi_g(2)$ | 27.5 | $^3\Pi_u$ | 30.2 |
| $^3\Pi_g(1)$ | 25.1 | $^3\Pi_u(1)$ | 27.5 | $^1\Sigma_g$ | 30.2 |
| $^3\Sigma_u^+(1)$ | 25.2 | $^1\Pi_u(1)$ | 27.6 | $^1\Pi_u$ | 31.5 |
| $^1\Pi_g(1)$ | 25.5 | $^3\Sigma_u^+(2)$ | 27.7 | $^1\Pi_g$ | 32.4 |
| $^1\Sigma_u^+(1)$ | 25.5 | $^1\Sigma_u^+(2)$ | 27.8 | $^3\Pi_g$ | 32.5 |
| $^3\Sigma_g^+(1)$ | 26.8 | $^3\Sigma_g^+(2)$ | 28.1 | $^3\Sigma_g$ | 33.0 |
| $^1\Sigma_g^+(2)$ | 27.2 | $^3\Pi_u(2)$ | 28.2 | $^3\Sigma_u$ | 33.0 |
| $^3\Pi_g(2)$ | 27.4 | $^1\Pi_u(2)$ | 28.2 | $^1\Sigma_u^+$ | 33.3 |

[a] The thresholds are the energies of the autoionizing states at $R = 1.8a_0$ above $v'' = 0$ of $X\,^1\Sigma_g^+$. $R = 1.8a_0$ is near the large $R$ turning point of $v'' = 0$. The threshold for $H_2^+\,^2\Sigma_u^+$ is 29.1 eV and for $^2\Pi_u$ is 34.9 eV.

agreement with the value reported here, $E=-0.10162$ (see Table IV). Dastidar and Dastidar[55] have reported a single configuration calculation for $Q_1\,{}^1\Sigma_g^+$ in a Slater basis set. The reported[55] energy (see Table IV) at $R=1.6$ is 0.4 eV above that reported here.

The $Q_1\,{}^3\Sigma_u^+(1)$ potential agrees well with previous results[42] being about 0.06 eV below the previous result in the Franck–Condon region.

The $Q_1\,{}^1\Sigma_u^+(1)$ state reported by O'Malley[35] uses the same definition for the projection operators as that used here but is a small three configuration calculation.

The $Q_1\,{}^3\Pi_u(1)$ state has been reported previously[42] although mislabeled as $Q_1\,{}^3\Pi_g$. $Q_1\,{}^3\Pi_u(1)$ and $Q_2\,{}^3\Pi_u$ have a crossing near $R=1.0\,a_0$. Comparison of Tables IV and V shows that the previously[42] reported $Q_1\,{}^3\Pi_u(1)$ state may have been a $Q_2$ state at $R=1.0$ and $R=1.2\,a_0$.

There have been two previous calculations of the ${}^1\Pi_u(2)$ state. The current results are in excellent agreement (differing by no more than 0.01 eV) with the potential curve of Hazi[38] obtained with the stabilization method. However, Bottcher's[40] potential curve is 1.3 eV above both the previous[38] and current results at $R=1.4\,a_0$. The discrepancy increases as $R$ increases. Bottcher's result lies above the ${}^2\Sigma_u^+$ state and is clearly unreliable as has been previously discussed by Hazi.[38] Indeed Bottcher's ${}^1\Pi_u(2)$ state resembles the $Q_2\,{}^1\Pi_u$ state calculated here and by Bottcher at $R=1.0$ and $1.2\,a_0$. The ${}^1\Pi_u(1)$ state at $R=2.0\,a_0$ has recently been reported at $E=25.62$ eV above $v=0$ of $X\,{}^1\Sigma_g^+$ by Hazi and Robb.[34] This is in excellent agreement with the current result of 25.627 eV. The current results for $Q_2\,{}^1\Pi_u$ agree well with the previous results[40] in the Franck–Condon region but are about 0.5 eV above the previous results at $R=6.0\,a_0$. This may be due to the optimization of the current basis set at $R=1.4\,a_0$.

Calculations of the positions and widths of seven doubly excited states from the phase shifts determined by the Kohn variational principle have been reported by Takagi and Nakamura at $R=2.0a_0$.[43] For the $Q_1\,{}^1\Sigma_u^+(1)$, ${}^1\Sigma_u^+(2)$, ${}^3\Sigma_u^+(1)$, and ${}^3\Sigma_u^+(2)$ states the reported energies are $-0.2892$, $-0.2055$, $-0.2987$, and $-0.2077$ hartree respectively. The states calculated here (see Table IV) are in good agreement with these results. For roots 1 and 2 of each of the above symmetries the states calculated here are about 0.1 eV and 0.2 eV respectively, lower than those reported by Takagi and Nakamura.[43] For $Q_2\,{}^3\Pi_u$ an energy of $-0.0969$ hartree was reported[43] which is only 0.05 eV above the energy reported here (see Table IV). For $Q_2\,{}^1\Pi_u(1)$ and $Q_2\,{}^1\Pi_u(2)$ energies of $-0.1365$ and $-0.0578$ hartree were reported.[43] The latter energy is 0.2 eV below the $Q_2\,{}^1\Pi_u(1)$ state calculated here. The reported[43] $Q_2\,{}^1\Pi_u(1)$ state cannot be energetically associated with any ${}^1\Pi_u$ state reported here. In addition the reported[43] $Q_2\,{}^1\Pi_u(1)$ state surprisingly lies 1.1 eV below the corresponding $Q_2\,{}^3\Pi_u$ state. Therefore it appears that the assignment of $Q_2\,{}^1\Pi_u(1)$ by these authors[43] to an apparent resonance in $p$ wave scattering found at $-0.1365$ hartree is incorrect.

In recent theoretical studies[56–58] of dissociative recombination of $H_2^+$ to $n\geq 3$ atoms the energies of the $Q_1$ states have been approximated as the sum of the exact $1\sigma_u$ energy and the hydrogenic binding energy of $-1/2n^2$ for the outer orbital. While the $\Sigma_u$ states[56,57] arising from $n=3$ have not been calculated here, comparison can be made to the $\Pi_{g,u}$ states arising from $n=3$. The energies of the $Q_1\,{}^3\Pi_u(2)$ and $Q_1\,{}^1\Pi_u(2)$ states are higher than that predicted from the above sum by 0.64 and 0.67 eV, respectively, while the $Q_1\,{}^3\Pi_g(2)$ and $Q_1\,{}^1\Pi_g(2)$ states are lower by 0.19 and 0.10 eV, respectively. As a result caution must be exercised in using the above sum to represent the $Q_1$ states. Potential curve displacements of the order of 0.6 eV can lead to very large errors in dissociative recombination cross sections from particular ion vibrational levels.

## V. COMPARISON TO EXPERIMENTAL RESULTS

The potential curves described here provide routes for dissociative ionization of $H_2$ by photon and electron impact, predissociation of excited vibrational levels of high Rydberg states, and dissociative recombination of $H_2^+$.

### A. Dissociative photoionization

The work of Browning and Fryar[7,8] on dissociative photoionization has been described in the Introduction. As can be seen from Table VI the only optically allowed state near 26 eV is ${}^1\Sigma_u^+(1)$. ${}^1\Pi_u(1)$ is accessible at 27.6 eV but has a dipole transition moment[51] from the ground state of 0.0271 a.u. at $R=1.8\,a_0$ which is 29% of the transition moment (0.0919 a.u.) to ${}^1\Sigma_u^+(1)$ leading to an excitation cross section (neglecting vibration) which is about 17% of that for ${}^1\Sigma_u^+(1)$. ${}^1\Sigma_u^+(2)$ is accessible at 27.8 eV and has a dipole transition moment[51] of 0.0775 at $R=1.8\,a_0$ and an excitation cross section which is about 71% of that for ${}^1\Sigma_u^+(1)$. The last calculated accessible $Q_1$ state is ${}^1\Pi_u(2)$ which has a transition moment[51] of 0.0174 at $R=1.8$ and an excitation cross section which is about 7% of the ${}^1\Sigma_u^+(1)$ cross section. Therefore, beneath the ${}^2\Sigma_u^+$ state the ${}^1\Sigma_u^+(1)$ and ${}^1\Sigma_u^+(2)$ states may play the dominant roles in photon excitation. Calculations[13] using the ${}^1\Sigma_u^+(1)$ state reported here and a quantal description of the nuclear motion yield 0.031 for the $H^+/H_2^+$ ratio, which is in excellent agreement with the results of Browning and Fryar (0.025) at 26.9 eV. Fryar and Browning[8] have reported an $H^+/H_2^+$ ratio of $0.108\pm0.024$ using 40.8 eV photons. However, at this photon energy the ${}^2\Sigma_u^+$ and higher $H_2^+$ states are accessible in addition to the $Q_2\,{}^1\Sigma_u^+$ and ${}^1\Pi_u$ states reported here.

Strathdee and Browning[11] have reported measurements of the proton kinetic energy distribution using 19.8 and 26.9 eV photons. With 19.8 eV photons they only observed protons with kinetic energies less than 1 eV. These protons arise from dissociation along the repulsive wall of $X\,{}^2\Sigma_g^+$. However, at 26.9 eV they observed protons with kinetic energies between 2 and 4.4 eV peaking near 3.5 eV. They assigned this peak to autoionization through the $Q_1\,{}^1\Sigma_u^+$ state. Calculations referred to above[13] using $^1\Sigma_u^+(1)$ reported here reproduce this peak leaving little doubt as to the source of the 2–4.4 eV protons. A recent paper[12] gives experimental results for 30.5 and 40.8 eV photons. At 30.5 eV the $H^+$ intensity peaks in the 4–5 eV region and extends to about 6 eV. By conservation of energy, protons are expected with energies up to 6.2 eV. At 30.5 eV in addition to $^1\Sigma_u^+(1)$ we would also expect to populate $^1\Sigma_u^+(2)$ (accessible at about 27.8 eV) based on the calculated dipole moments. However, the vibrational continuum function for $^1\Sigma_u^+(1)$ has a greater overlap with the $v = 0$ $H_2$ ground state vibrational wave function than for $^1\Sigma_u^+(2)$ at 30.5 eV. Using a $\delta$ function for the vibrational continuum wave function we estimate that the cross section for populating $^1\Sigma_u^+(2)$ is about 46% of that for populating $^1\Sigma_u^+(1)$ at these energies. Therefore, at 30.5 eV both $^1\Sigma_u^+(1)$ and $^1\Sigma_u^+(2)$ will be important autoionization routes in photon excitation. A more definitive statement here requires calculation of the $^1\Sigma_u^+(2)$ autoionization widths. Note that dipole allowed $Q_2$ states are not accessible at 30.5 eV. The $^2\Sigma_u^+$ state, which can be expected to play an important role at this energy, will, however, not contribute to the oscillatory nature of the proton spectra. Using a quantal distribution of the nuclear motion and only the $^1\Sigma_u^+(1)$ state reported here, qualitative agreement has been obtained with the 30.5 eV experimental proton spectra.[13,59] However, it would be of interest to include the $^1\Sigma_u^+(2)$ state reported here in these calculations. At 40.8 eV several autoionizing states and states of $H_2^+$ can provide direct routes for dissociative photoionization. Predictions of the proton spectra expected at this energy are not possible without detailed calculations of dissociative photoionization through the accessible $H_2^+$ channels.

Two recent experiments involving the detection of forward scattered high energy electrons with little momentum transfer have measured photoionization oscillator strengths. The $H^+/H_2^+$ ratios for photon energies reported by Backx *et al.*[31] below 30 eV are in excellent agreement with the results of Browning and Fryar.[7] Backx *et al.*[31] report a large contribution to $H^+$ production near the threshold of the $^2\Sigma_u^+$ ion state. Also their measured ionization efficiency shows a dip near 37 eV which they attribute to a $Q_2\,^1\Pi_u$ state (previously identified by Misakian and Zorn[23] with a threshold of 32 eV) which dissociates to $H(2s) + H(2p)$. From Table VI and Fig. 1 we see that $Q_2\,^1\Pi_u$ has a threshold of 31.5 eV and crosses $^2\Sigma_u$ at about 35 eV. Hazi *et al.*[34] have studied this state and predict (using a classical treatment) that 90% of the $Q_2\,^1\Pi_u$ state dissociates to neutrals supporting the dip seen in the measured ionization efficiency of Backx *et al.*[31] Note that at energies near 37 eV, $Q_2\,^1\Sigma_u^+$ with a threshold of 33.3 eV (Table VI), may need to be considered. van Wingerden *et al.*[32] have also reported optical oscillator strengths from electron impact experiments. For photon energies up to 30 eV they report agreement with Strathdee and Browning for the kinetic energy distribution of atomic ions and for the cross section for production of $D^+$ with kinetic energies above 2 eV. At 35 eV they report a $D^+$ distribution surprisingly centered around 1 eV which they attribute to $Q_2\,^1\Pi_u$.

### B. Electron impact

Kollmann[10] has recently reported threshold energies for proton production resulting from electron impact. He finds three distinct thresholds at $E^{I} = 23.5 \pm 0.7$ eV, $E^{II} = 26.1 \pm 0.5$ eV, and $E^{III} = 27.7 \pm 0.6$ eV each of which leads to dissociative ionization. This is in good agreement with the discussion of Sec. III in which it was shown that the autoionizing states fall into three distinct groups. From Sec. III and Table VI we see that $E^{I}$ corresponds to $^1\Sigma_g^+(1)$. In the range of $E^{II}$ we have $^1\Pi_g(1)$ and $^1\Sigma_u^+(1)$. However, it is also possible that the $^3\Sigma_u^+(1)$ and $^3\Pi_g(1)$ states may make some contribution to $E^{II}$ at threshold energies. Note that the threshold energies in Table VI are only for $R = 1.8\ a_0$. The third group of states discussed previously includes all the remaining $Q_1$ states calculated here. All of the members of this third group fall within the range of $E^{III}$ except for $^3\Sigma_g^+(1)$ (see Table VI). The proton distribution found by Kollmann resembles that found by Strathdee and Browning near 26.9 eV but does not reproduce the peaks found by Crowe and McConkey.[30] However $E^{I}$ and $E^{II}$ agree with thresholds reported by Crowe and McConkey. Stockdale *et al.*[27] also did not reproduce the peaks reported by Crowe and McConkey[30] for electron energies less than 40 eV. However Stockdale *et al.*[27] did not find evidence for states leading to $D^+$ production in the region between 19 and 32 eV.

Landau *et al.*[29] have reported five threshold regions for $H^+$ production in electron impact excitation: $22.3 \pm 0.5$, $23.9 \pm 0.3$, $25.8 \pm 0.3$, $26.9 \pm 0.3$, and $27.9 \pm 0.2$ eV. The results reported here show that $Q_1\,^1\Sigma_g^+$ is the only autoionizing state accessible in the Franck–Condon region at energies below 25 eV. Therefore, if the first two thresholds reported by Landau *et al.*[29] are due to autoionization they would have to be accounted for by $Q_1\,^1\Sigma_g^+$. However it is difficult to explain why two thresholds should be associated with a single autoionizing state. The authors[29] did not assign the 22.3 eV threshold to a particular process. The third reported threshold region was assigned[29] to $^3\Sigma_u^+$ in agreement with results reported here. However, as seen in Fig. 1, $^3\Sigma_u^+$ and $^3\Pi_g$ are nearly equal in energy and any observed threshold in this energy region in electron impact would be due to both of these states. The same can be said for the $^1\Sigma_u^+$ and $^1\Pi_g$ states. The proton energy distribution arising from photon impact[12] of $^1\Sigma_u^+$ was compared[29] with that arising from electron impact near 26.9 eV. However, because of the near degeneracy of $^1\Sigma_u^+$ and $^1\Pi_g$ (see Tables V and VI) both $^1\Sigma_u^+$ and $^1\Pi_g$ need to be considered in electron impact whereas $^1\Sigma_u^+$ is the only dipole allowed state at 26.9 eV. The partitioning of the highest two thresholds among the states reported in Table VI awaits the calculation of the widths and the cross sections for proton production from these states.

In electron impact experiments Misakian and Zorn[23] have found that a threshold for production of $H(2s)$ atoms with a kinetic energy of 3.8 eV occurs at 32 eV while production of 2 eV $H(2s)$ has a threshold of 29 eV. This appears to be consistent with a doubly excited state dissociating to the $n = 2 + n = 2$ limit. From the deduced asymptotic energy and the angular distribution of H(2*s*) Misakian and Zorn conclude that the state has $^1\Pi_u$ symmetry. This state corresponds to the $Q_2\,{}^1\Pi_u$ state which has a calculated threshold of 31.5 eV (see Table VI) and is too high to account for the 29 eV threshold. Table VI shows that there is a $Q_2\,{}^1\Sigma_g^+$ threshold near 30.2 eV. This state has the same asymptotic energy as $Q_2\,{}^1\Pi_u$ and will contribute to the 3.8 eV H(2*s*) atoms at the 32 eV threshold. They also observe slow H(2*s*) atoms which they attribute to lower "singly excited" states of $H_2$. They disagree with an earlier conclusion of Czarnik and Fairchild[22] that doubly excited $^1\Sigma_u^+$ states can predissociate the $8p\sigma\,{}^1\Sigma_u^+$ ($v = 5$) Rydberg state leading to slow (<1 eV) H(2*s*) atoms. From Fig. 1 it is apparent that $^1\Sigma_u^+(1)$ is too high by about 0.7 eV to lead to predissociation of the $v = 5$ level of this high $^1\Sigma_u^+$ Rydberg state.

Spezeski, Kalman, and McIntyre[26] have reported electron impact studies of $H_2$ and $D_2$ and the resulting time of flight distribution of H(2*s*) and D(2*s*) detected at right angles to the electron beam. At 27 eV electron impact energy they detect a 2.7 eV H(2*s*) peak which they attribute to $Q_1\,{}^1\Sigma_g^+(1)$ in agreement with results reported here. Table VI shows that $Q_1\,{}^1\Sigma_g^+(2)$ is also accessible near 27 eV and may contribute to the 2.7 eV peak. At 38 eV an H(2*s*) peak centered near 3.5 eV was attributed to $Q_2\,{}^1\Pi_u$ in accord with the results reported here. However, as pointed out above, a $Q_2\,{}^1\Sigma_g^+$ state with threshold at 30.2 eV (see Table VI) dissociating to two H(2*s*) atoms must also be considered.

Schiavone, Smyth, and Freund[24] have reported production of high Rydberg fragment atoms from electron impact excitation. One group of Rydberg atoms has a production threshold near 23 eV and was identified with the excitation of $Q_1\,{}^1\Sigma_g^+$ (see Table VI and Fig. 1). As this state dissociates it can cross over into Rydberg bound states (having the ground state of $H_2^+$ as core) leading to dissociation to energetic high Rydberg atoms. Since the Rydberg atoms were detected at 90° to the electron beam the $^1\Sigma_g^+$ and $^1\Pi_u\,Q_1$ states will be important. Near 27.6 eV (see Table VI) the $Q_1\,{}^1\Pi_u(1)$ state should begin to contribute to Rydberg atom production.

Ogawa and Higo[15] report high resolution measurements of the Balmer-$\beta$ line shape of H* resulting from electron impact excitation of $H_2$. They report a threshold for fast H* at $24 \pm 1$ eV which was attributed to the lowest $Q_1\,{}^1\Sigma_g^+$ state in agreement with the results reported here. An additional threshold reported near 27 eV may be due to $^1\Sigma_g^+(2)$ and additional states discussed above and shown in Table VI.

### C. Dissociative recombination

Experimental measurements of $H_2^+$ and $D_2^+$ dissociative recombination have been performed with perpendicular,[60,61] inclined,[62,63] and merged[64–66] electron and $H_2^+$ beams and with an ion trap.[67] The experiments have yielded cross sections for total[62–66] recombination and for recombination into the $n = 2$ and $n = 4$ atomic states.[60,61] The theoretical determination of dissociative recombination cross sections for the $Q_1$ states shown in Fig. 1 awaits the calculation of widths and vibrational wave functions. Some implications of the current results for dissociative recombination have already been discussed in Sec. IV. From Fig. 1 we see that dissociative recombination from $v = 0$ is expected to have a small cross section. An important feature of the experiments is that they involve vibrationally excited ions with the peak population in $v = 1$ for $H_2^+$ and $v = 2$ for $D_2^+$. Furthermore the experiments indicate that recombination to highly excited atoms may account for most of the total recombination cross section[60,61] and recombination of vibrational levels with $v > 2$ is very important.[64,65] These results indicate that the $Q_1\,\Sigma_u^+$ and $Q_1\,\Pi_g(1)$ states may also play an important role.

A complete discussion of $H_2^+$ dissociative recombination should also consider the role played by the singly excited $^1\Sigma_u^+$ state which arises from the $H^+ + H^-$ asymptote.[68] This state may cross the ground state of $H_2^+$ between the turning points of $v = 0$ and is expected to have a large width.

## ACKNOWLEDGMENTS

The author is grateful to Professor A. Dalgarno for suggesting this study and for many helpful discussions. This work was supported at Harvard by the Atmospheric Sciences Section of the National Science Foundation and at Boston College by NASA Ames Grant No. NAG2-89 and Air Force Geophysics Laboratory Contract No. F19628-79-C-0139.

[1]T. E. Cravens, G. A. Victor, and A. Dalgarno, Planet. Space Sci. **23**, 1059 (1975).
[2]W. T. Huntress, Jr., Adv. Atom. Mol. Phys. **10**, 295 (1974).
[3]P. M. S. Blackett and J. Franck, Z. Phys. **34**, 389 (1925).
[4]M. Leventhal, R. T. Bobiscoe, and K. R. Lea, Phys. Rev. **158**, 49 (1967).
[5]W. E. Lamb, Jr. and R. C. Retherford, Phys. Rev. **79**, 549 (1950).
[6]L. J. Kieffer and G. H. Dunn, Phys. Rev. **158**, 61 (1967).
[7]R. Browning and J. Fryar, J. Phys. B **6**, 364 (1973).
[8]J. Fryar and R. Browning, Planet. Space Sci. 21, 709 (1973).
[9]A. L. Ford, K. K. Docken, and A. Dalgarno, Astrophys. J. **185**, 819 (1975).
[10]K. Kollmann, J. Phys. B **11**, 339 (1978).
[11]S. Strathdee and R. Browning, J. Phys. B **9**, L505 (1976).
[12]S. Strathdee and R. Browning, J. Phys. B **12**, 1789 (1979).
[13]K. Kirby, S. Guberman, and A. Dalgarno, J. Chem. Phys. **70**, 4635 (1979).
[14]M. Higo and T. Ogawa, Chem. Phys. Lett. **75**, 271 (1980).
[15]T. Ogawa and M. Higo, Chem. Phys. **52**, 55 (1980).
[16]M. Higo and T. Ogawa, Chem. Phys. **56**, 15 (1981).
[17]R. S. Freund, J. A. Schiavone, and D. F. Brader, J. Chem. Phys. **64**, 1122 (1976).
[18]M. Glass-Maujean, J. Phys. B **11**, 431 (1978).
[19]G. R. Mohlmann, F. J. de Heer, and J. Los, Chem. Phys. **25**, 103 (1977).
[20]C. Karolis and E. Harting, J. Phys. B **11**, 357 (1978).
[21]G. A. Khayrallah, Phys. Rev. A **13**, 1989 (1976).
[22]J. W. Czarnik and C. E. Fairchild, Phys. Rev. Lett. **26**, 807 (1971).
[23]M. Misakian and J. C. Zorn, Phys. Rev. **6**, 2180 (1972).
[24]J. A. Schiavone, K. C. Smyth, and R. S. Freund, J. Chem. Phys. **63**, 1043 (1975).
[25]B. L. Carnahan and E. C. Zipf, Phys. Rev. A **16**, 991 (1977).
[26]J. J. Spezeski, O. F. Kalman, and L. C. McIntyre, Jr., Phys. Rev. A 22, 1906 (1980).

[27]J. A. D. Stockdale, V. E. Anderson, A. E. Carter, and L. Deleanu, J. Chem. Phys. **63**, 3886 (1975).
[28]K. Kollmann, Int. J. Mass. Spectrosc. Ion Phys. **17**, 261 (1975).
[29]M. Landau, R. I. Hall, and F. Pichou, J. Phys. B **14**, 1509 (1981); M. Landau, R. I. Hall, F. Pichou, and C. Schermann, Phys. Lett. A **89**, 75 (1982).
[30]A. Crowe and J. W. McConkey, Phys. Rev. Lett. **31**, 192 (1973); J. Phys. B **6**, 2088 (1973).
[31]C. Backx, E. R. Wright, and M. J. Van der Wiel, J. Phys. B **9**, 315 (1976).
[32]B. Van Wingerden, Ph. E. van der Leeuw, F. J. de Heer, and M. J. van der Wiel, J. Phys. B **12**, 1559 (1979).
[33]N. Bose, J. Phys. B **11**, L309 (1978).
[34]A. U. Hazi in *Electron–Molecule and Photon–Molecule Collisions*, edited by T. Rescigno, V. McKoy, and B. Schneider (Plenum, New York, 1978), p. 281.
[35]T. O'Malley, J. Chem. Phys. **51**, 322 (1969).
[36]A. U. Hazi, Chem. Phys. Lett. **25**, 259 (1974).
[37]A. U. Hazi, J. Chem. Phys. **60**, 4358 (1974).
[38]A. U. Hazi, J. Phys. B **8**, L262 (1975).
[39]A. U. Hazi and K. Wiemers, J. Chem. Phys. **66**, 5296 (1977).
[40]C. Bottcher, J. Phys. B **7**, L352 (1974).
[41]C. Bottcher, J. Phys. B **9**, 2899 (1976).
[42]C. Bottcher and K. Docken, J. Phys. B **7**, L5 (1974).
[43]H. Takagi and H. Nakamura, J. Phys. B **13**, 2619 (1980).
[44]H. Feshbach, Ann. Phys. (N.Y.) **5**, 357 (1958); R. H. Lemmer, Rep. Prog. Phys. **29**, 131 (1966).
[45]T. F. O'Malley and S. Geltman, Phys. Rev. **137**, 1344 (1965).
[46]T. F. O'Malley, Phys. Rev. **150**, 14 (1966).
[47]E. Hylleraas, Z. Phys. **65**, 759 (1930); J. K. McDonald, Phys. Rev. **43**, 830 (1933).
[48]S. Huzinaga, J. Chem. Phys. **42**, 1293 (1965).
[49]C. B. Wakefield and E. R. Davidson, J. Chem. Phys. **43**, 834 (1965).
[50]The two roots of each symmetry are denoted by a (1) or (2) following the state symbol.
[51]S. L. Guberman (unpublished results).
[52]L. Wolniewicz and K. Dressler, J. Mol. Spectrosc. **67**, 416 (1977).
[53]E. R. Davidson, J. Chem. Phys. **35**, 1189 (1961).
[54]N. Moiseyev and C. T. Corcoran, Phys. Rev. A **20**, 814 (1979).
[55]K. R. Dastidar and T. K. R. Dastidar, J. Phys. Soc. Jpn **46**, 1288 (1979).
[56]V. P. Zhdanov and M. I. Chibisov, Sov. Phys. JETP **47**, 38 (1978).
[57]C. Derkits, J. N. Bardsley, and J. M. Wadehra, J. Phys. B **12**, L529 (1979).
[58]V. P. Zhdanov, J. Phys. B **13**, L311 (1980).
[59]K. Kirby, T. Uzer, A. C. Allison, and A. Dalgarno, J. Chem. Phys. **75**, 2820 (1981).
[60]R. A. Phaneuf, D. H. Crandall, and G. H. Dunn, Phys. Rev. A **11**, 528 (1975).
[61]M. Vogler and G. H. Dunn, Phys. Rev. A **11**, 1983 (1975).
[62]B. Peart and K. T. Dolder, J. Phys. B **7**, 236 (1974).
[63]B. Peart and K. T. Dolder, J. Phys. B **6**, L359 (1973).
[64]J. Wm. McGowan, R. Caudano, and J. Keyser, Phys. Rev. Lett. **36**, 1447 (1976).
[65]J. Wm. McGowan, P. M. Mul, V. S. D'Angelo, J. B. A. Mitchell, P. Defrance, and H. R. Froelich, Phys. Rev. Lett. **42**, 373 (1979).
[66]D. Auerbach, R. Cacak, R. Caudano, T. D. Gaily, C. J. Keyser, J. Wm. McGowan, J. B. A. Mitchell, and S. F. J. Wilk, J. Phys. B **10**, 3797 (1977).
[67]D. Mathur, S. U. Khan, and J. B. Hasted, J. Phys. B **11**, 3615 (1978).
[68]M. R. Herman and P. W. Langhoff, Chem. Phys. Lett. **82**, 242 (1981); J. C. Slater, *Quantum Theory of Molecules and Solids*, (Addison–Wesley, Reading, 1963), Vol. 1, p. 69; D. Mathur, Int. J. Mass. Spectrosc. Ion Phys. **40**, 235 (1981).